



ELSEVIER

International Journal of Mass Spectrometry 181 (1998) 151–157



# Ab initio molecular orbital study on the gas phase $S_N2$ reaction $F^- + CH_3Cl \rightarrow CH_3F + Cl^-$

Manabu Igarashi, Hiroto Tachikawa\*

*Division of Molecular Chemistry, Graduate School of Engineering, Hokkaido University, Sapporo 060-8628, Japan*

Received 27 July 1998; accepted 11 September 1998

## Abstract

Ab-initio molecular orbital (MO) and direct ab initio dynamics calculations have been applied to the gas phase  $S_N2$  reaction  $F^- + CH_3Cl \rightarrow CH_3F + Cl^-$ . Several basis sets were examined in order to select the most convenient and best fitted basis set to that of high-quality calculations. The Hartree–Fock (HF)  $3-21+G(d)$  calculation reasonably represents a potential energy surface calculated at the  $MP2/6-311++G(2df,2pd)$  level. A direct ab initio dynamics calculation at the HF/ $3-21+G(d)$  level was carried out for the  $S_N2$  reaction. A full dimensional ab initio potential energy surface including all degrees of freedom was used in the dynamics calculation. Total energies and gradients were calculated at each time step. Two initial configurations at time zero were examined in the direct dynamics calculations: one is a near collinear collision, and the other is a side-attack collision. It was found that in the near collinear collision almost all total available energy is partitioned into two modes: the relative translational mode between the products ( $\sim 40\%$ ) and the C – F stretching mode ( $\sim 60\%$ ). The other internal modes of  $CH_3F$  were still in the ground state. The lifetimes of the early- and late-complexes  $F^- \cdots CH_3Cl$  and  $FCH_3 \cdots Cl^-$  are significantly short enough to dissociate directly to the products. On the other hand, in the side-attack collision, the relative translation energy was about 20% of total available energy. (Int J Mass Spectrom 181 (1998) 151–157) © 1998 Elsevier Science B.V.

*Keywords:*  $S_N2$  reaction; Ab initio molecular orbital (MO) calculation; Direct ab initio dynamics; Energy distribution

## 1. Introduction

The classical trajectory method has been used for elucidating the chemical reaction because it is a convenient and powerful tool for understanding chemical reaction dynamics [1,2]. In general, classical trajectories are calculated on an analytical potential energy surface that is generally constructed by a fit to potential energy surface (PES) obtained from ab initio molecular orbital (MO) calculations for a large number of geometrical configurations, as previously car-

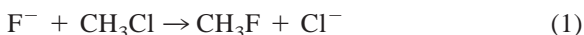
ried out by us [2]. However, it is still difficult to apply such a procedure to general polyatomic reaction systems because of the large number of degrees of freedom.

An alternative approach is to calculate the classical trajectories directly, utilizing the ab initio MO method without construction of the potential energy surface. This is called “direct ab initio dynamics calculation.” Recently, we developed a program code for a direct ab initio dynamics method and applied it to several reaction systems [3]. The direct ab initio dynamics method is thus a powerful tool. However, a weak point of the direct ab initio dynamics method is that it generally needs a large CPU time to generate even one

\* Corresponding author.

trajectory. Therefore, the smallest basis set is required for calculating PES. In addition, it is also required that the smallest basis set chosen in the calculation should reasonably represent the results of large basis sets and post-Hartree–Fock (HF) calculations. Therefore, a large number of pre-ab initio energetics calculations is needed before the dynamics calculation.

In the present work, we have first examined ab initio MO calculations with several basis sets for a nucleophilic substitution reaction of the  $S_N2$  type,



The most reasonable basis set to represent the PES was determined by means of the ab initio MO calculation. Second, a direct ab initio dynamics calculation was carried out by using the selected basis set. The dynamics and energy partitioning of reaction (1) were discussed on the basis of theoretical results.

For this reaction, several theoretical works have been made by using ab initio MO and classical trajectory calculations [4–21]. In these works, the dimension of the reaction system is reduced to a low mode. Full dimensional dynamics is scarcely known. The direct dynamics method would give useful information on a detailed dynamics of reaction (1).

## 2. Method of calculation

All ab initio molecular orbital calculations were carried out using the GAUSSIAN 94 program system [22] running on an IBM RS6000 work station. A range of different basis sets was tested from split valence plus polarization 3–21G(*d*) to large and flexible sets like 6–31++G\*\* with sets of polarization functions. Also considered were Dunning basis sets D95++\*\*.

By using the most reasonable basis set determined by these ab initio MO calculations [that is 3–21+G(*d*) basis set], we have made a direct ab initio MO dynamics calculation for reaction (1). The details of the dynamics calculations are described elsewhere [3]. The essence only is described in this section.

The HF/3–21+G(*d*) optimized geometry of  $CH_3Cl$  was chosen as an initial structure. At the start of the trajectory calculation, atomic velocities of  $CH_3Cl$  were

adjusted to give a temperature of 10 K. The classical Hamiltonian equation was numerically solved by the Runge–Kutta method. No symmetry restriction was applied to the calculation of the gradients. The time step size was chosen as 0.2 fs, and a total of 5000 steps were integrated for each dynamics calculation. The drift of the total energy is confirmed to be less than 2% at all steps in the trajectory.

## 3. Results and discussion

### 3.1. Ab initio MO study: geometries and energetics for the stationary points

In order to elucidate the energetics of reaction (1), the total energies for reactant and product states,  $F^- + CH_3Cl$  and  $FCH_3 + Cl^-$ , are calculated by several methods. The reaction energies ( $\Delta H$ 's) are also calculated by the total energies. The results of the values are listed in Table 1 together with the previously reported values. The  $-\Delta H$ 's calculated by the Hartree–Fock (HF) level of theory with several basis sets are much larger than the experimental values ( $34.0 \text{ kcal mol}^{-1}$ ) and more sophisticated calculations ( $31.32\text{--}34.61 \text{ kcal mol}^{-1}$ ) except for the HF/3–21+G(*d*) calculation ( $34.28 \text{ kcal mol}^{-1}$ ). The agreement of the 3–21+G(*d*) basis set with experimental values is attributed to the fact that the diffuse functions added to the halogen atoms ( $F^-$  and  $Cl^-$ ) cause an energy reduction.

The relative energies and geometries at the stationary points along the reaction coordinate for reaction (1) are summarized in Table 2. The zero level in the relative energy corresponds to the reactant state ( $F^- + CH_3Cl$ ). It was found that the energies for the early- and late-intermediate complexes calculated by HF/3–21+G(*d*) are in excellent agreement with those of MP2 and QCISD(T) calculations with the 6–31++G(2*df*,2*pd*) basis set. In addition, the energy of the saddle point was also in good agreement. As clearly indicated in Table 2, the HF/3–21+G(*d*) calculations for geometries and relative energies at the stationary points represent excellently those of the more sophisticated calculations.

Table 1

Total energies (in hartrees) and heats of reactions (in kcal mol<sup>-1</sup>) for the F<sup>-</sup> + CH<sub>3</sub>Cl → CH<sub>3</sub>F + Cl<sup>-</sup> reaction system

Method	F <sup>-</sup> + CH <sub>3</sub> Cl	Cl <sup>-</sup> + CH <sub>3</sub> F	ΔH
HF/3-21G*	-595.5671318	-595.7260126	-99.70
HF/3-21+G*	-595.7348354	-595.7894663	-34.28
HF/6-31G*	-598.4436346	-598.5606122	-73.40
HF/6-31+G*	-598.5124778	-598.5827830	-44.12
HF/6-31++G**	-598.5175352	-598.5888285	-44.74
HF/D95*	-598.5061597	-598.5790848	-45.76
HF/D95+*	-598.5370348	-598.6109698	-46.40
HF/D95**	-598.5113772	-598.5840266	-45.59
HF/D95++**	-598.5422953	-598.6160268	-46.27
<sup>a</sup> MP2/6-311++G(2df,2pd)			-31.32
<sup>a</sup> QCISD/6-311++G(2df,2pd)			-34.61
<sup>a</sup> QCISD(T)/6-311++G(2df,2pd)			-33.54
<sup>a</sup> CCSD(T)/vtz+2			-32.41
<sup>a</sup> G2(+)			-31.42

<sup>a</sup>Relative energies cited from the reference: H. Wang, W.L. Hase, J. Am. Chem. Soc. 119 (1997) 3093.

### 3.2. Harmonic vibrational frequencies

As shown in the previous section, the HF/3-21+G(*d*) level of theory gave a reasonable value for the geometries and relative energies in reaction (1). In this section, the harmonic vibrational frequencies at the

stationary points are compared. The results of the HF/3-21+G(*d*) calculations are listed in Table 3. The vibrational frequencies calculated at the HF/3-21+G(*d*) level were in good agreement with the experimental values and the results of the most sophisticated calculations.

Table 2

Ab initio geometries and relative energies ( $E_{\text{rel}}$  in kcal mol<sup>-1</sup>) for stationary points on the reaction path: bond lengths and angles are in Å and degrees, respectively

	<i>r</i> (C-F)	<i>r</i> (C-Cl)	<i>r</i> (C-H)	∠Cl-C-H	∠H-C-H	$E_{\text{rel}}$
F + CH <sub>3</sub> Cl reactants						
HF/3-21+G( <i>d</i> )	∞	1.806	1.076	108.2	110.7	0.0
MP2 <sup>a</sup>	∞	1.778	1.083	108.6	110.3	0.0
QCISD(T)						0.0
F...CH <sub>3</sub> Cl complex						
HF/3-21+G( <i>d</i> )	2.481	1.904	1.068	106.4	112.3	-15.8
MP2	2.511	1.837	1.077	108.1	110.8	-15.8
QCISD(T)						-16.6
[F...CH <sub>3</sub> Cl] <sup>-</sup> saddle point						
HF/3-21+G( <i>d</i> )	2.170	2.139	1.061	98.0	118.1	-14.1
MP2	1.997	2.106	1.069	95.9	119.0	-11.6
QCISD(T)						-14.0
FCH <sub>3</sub> ...Cl <sup>-</sup> complex						
HF/3-21+G( <i>d</i> )	1.464	3.273	1.073	72.8	111.6	-45.4
MP2	1.413	3.178	1.082	70.9	109.9	-41.2
QCISD(T)						-43.4
FCH <sub>3</sub> +Cl <sup>-</sup> products						
HF/3-21+G( <i>d</i> )	1.434	∞	1.077	72.6	111.4	-34.3
MP2	1.383	∞	1.086	71.1	110.0	-31.3
QCISD(T)						-33.5

<sup>a</sup>MP2: MP2/6-311++G(2df,2pd).

Table 3  
Harmonic vibrational frequencies (in  $\text{cm}^{-1}$ ) for stationary points along the reaction path

Mode	HF/3-21+G(d)	MP2 <sup>a</sup>	Experimental <sup>b</sup>
F <sup>-</sup> + CH <sub>3</sub> Cl reactants			
A <sub>1</sub> , C-Cl str	717	769	740
E, CH <sub>3</sub> rock	1143	1042	1038
A <sub>1</sub> , CH <sub>3</sub> deform.	1542	1397	1383
E, CH <sub>3</sub> deform.	1653	1502	1482
A <sub>1</sub> , C-H str	3255	3120	3074
E, C-H str	3350	3232	3166
F <sup>-</sup> ... CH <sub>3</sub> Cl complex			
E, F <sup>-</sup> bend	131	78	
A <sub>1</sub> , F-C str	171	174	
A <sub>1</sub> , C-Cl str	470	612	
E, CH <sub>3</sub> rock	1087	966	
A <sub>1</sub> , CH <sub>3</sub> deform.	1433	1277	
E, CH <sub>3</sub> deform.	1605	1463	
A <sub>1</sub> , C-H str	3339	3186	
E, C-H str	3470	3317	
[F ... CH <sub>3</sub> ... Cl] <sup>-</sup> saddle point			
E, F-C-Cl bend	231	257	
A <sub>1</sub> , F-C-Cl str	277	305	
E, CH <sub>3</sub> rock	1079	1007	
A <sub>1</sub> , out-of-plane bend	1328	1151	
E, CH <sub>3</sub> deform.	1555	1427	
A <sub>1</sub> , C-H str	3386	3224	
E, C-H str	3573	3422	
reaction coordinate	373 i	501 i	
FCH <sub>3</sub> ... Cl <sup>-</sup> complex			
E, Cl <sup>-</sup> bend	108	94	
A <sub>1</sub> , C-Cl str	103	113	
A <sub>1</sub> , F-C str	972	989	
E, CH <sub>3</sub> rock	1239	1165	
A <sub>1</sub> , CH <sub>3</sub> deform.	1571	1446	
E, CH <sub>3</sub> deform.	1638	1504	
A <sub>1</sub> , C-H str	3296	3138	
E, C-H str	3407	3255	
FCH <sub>3</sub> + Cl <sup>-</sup> products			
A <sub>1</sub> , F-C str	1075	1086	1077
E, CH <sub>3</sub> rock	1263	1211	1207
A <sub>1</sub> , CH <sub>3</sub> deform.	1611	1505	1496
E, CH <sub>3</sub> deform.	1653	1521	1514
A <sub>1</sub> , C-H str	3247	3097	3046
E, C-H str	3339	3199	3165

<sup>a</sup>MP2: MP2/6-311++G(2df,2pd).

<sup>b</sup>Experimental values are cited from [23] and [24].

### 3.3. Direct ab initio dynamics study

As indicated by the ab initio calculations with several basis sets, the HF/3-21+G(d) calculation

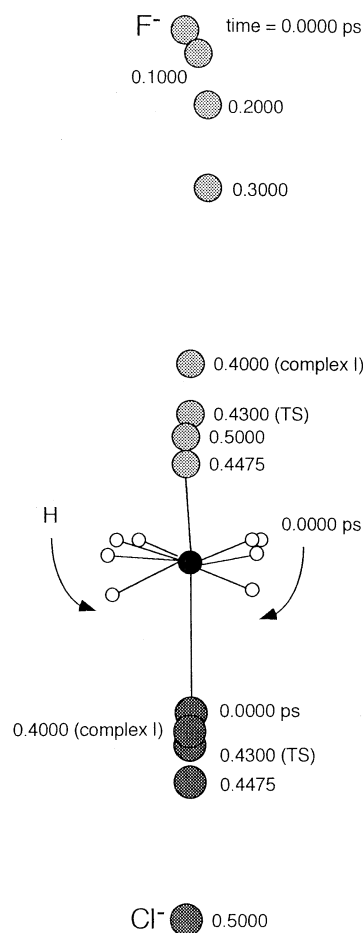


Fig. 1. Snapshots for a near collinear collision of reaction (1) illustrated as a function of time.

gave a reasonable PES for reaction (1). In this section, we shall attempt a direct ab initio dynamics calculation at the HF/3-21+G(d) level. The results for two collision angles (i.e. near collinear collision and side-attach collision) are given.

#### 3.3.1. Near collinear collision

A snapshot calculated for the near collinear collision is illustrated in Fig. 1. In this trajectory, the initial separation between the F<sup>-</sup> ion and the carbon atom of CH<sub>3</sub>Cl was chosen as 6.20 Å, and the angle of F-C-Cl was 179.8° at time zero. After the start of the trajectory, the bending angle of CH<sub>3</sub>Cl, ∠H-C-Cl, was still almost constant up to 0.38 ps. The F<sup>-</sup>

approached from a collinear direction with respect to the C–Cl bond. The H–C–Cl angle was suddenly varied at time 0.40 ps, suggesting that a Walden inversion takes place at this time regime. After that, the Cl<sup>-</sup> was rapidly ejected from the CH<sub>3</sub>F molecule, and the C–F bond was newly formed.

In order to elucidate the energetics during the reaction, total energy of the system was monitored. The results are given in Fig. 2(A). The potential energy shows that the reaction occurred over a very short time (<1.0 ps) and the reaction intermediates (early and late complexes, F<sup>-</sup> . . . CH<sub>3</sub>Cl and FCH<sub>3</sub> . . . Cl<sup>-</sup>, respectively) are formed in the wings of transition state. The lifetimes for both intermediates were short enough (<0.12 ps) to proceed nonstatistically. The reaction proceeds via a direct mechanism. The interatomic distances [Fig. 2(B)] clearly show that the bond breaking and formation take place at 0.40 ps. After the formation of the new C–F bond, the C–F stretching mode is vibrationally excited due to energy transfer to the C–F bond. The sudden change of the F–C–H angle indicates that a Walden inversion efficiently occurred at 0.40 ps. In the case of this sample trajectory, the total available energy is mainly partitioned into the relative translational energy (~40%) and the C–F stretching mode ( $\nu = 5$ ).

### 3.3.2. Side-attack collision

A snapshot calculated for a side-attack collision is illustrated in Fig. 3. The initial separation and collision angle at time zero were 6.38 Å and 150.3°, respectively. After the start of the trajectory, F<sup>-</sup> approached CH<sub>3</sub>Cl so as to depict a circle and then collided with CH<sub>3</sub>Cl from the collinear direction (time = 0.4065 ps). However, the substitution did not take place and the F<sup>-</sup> ion rebounded from CH<sub>3</sub>Cl. At 0.5750 ps, the F<sup>-</sup> ion was located 4.30 Å away from the carbon atom. After that, the F<sup>-</sup> ion again approached CH<sub>3</sub>Cl and collided into the carbon atom. After the second collision, the substitution had efficiently occurred.

The energies, interatomic distances, and angles for the side-attack collision are plotted in Fig. 4. The energy gradually dropped to -12 kcal mol<sup>-1</sup> by the first collision. This drop is attributed to the formation

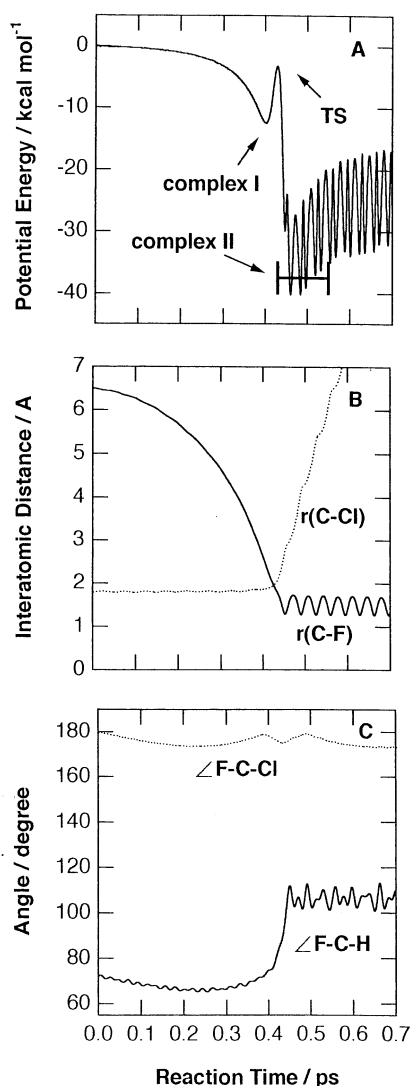


Fig. 2. Potential energy (A), interatomic distances (B), and angles vs. reaction time, calculated by the direct MO dynamics calculation (HF/3-21G+(*d*) level) for a near collinear collision of reaction (1).

of a collision complex. It should be noted that the excess energy of complex I is transferred efficiently to the C–Cl bond and the bending mode of CH<sub>3</sub>Cl despite having no reaction. A fine structure of potential energy appearing within 0.40–0.78 ps indicates the excitation of the C–Cl stretching mode. At the second collision, the trajectory reached the transition state for the substitution reaction (TS) and lead to

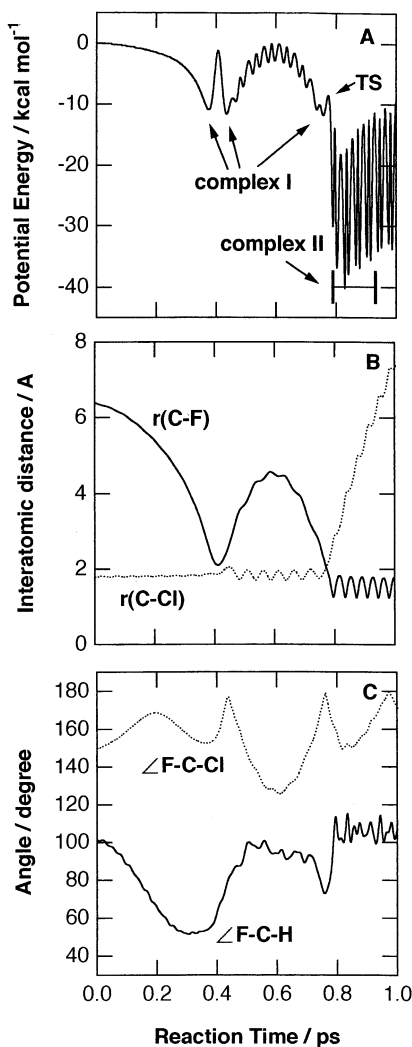


Fig. 3. Snapshots for a side-attack collision of reaction (1) illustrated as a function of time.

complex II. The lifetime of complex II is significantly short, thus suggesting that the late complex  $F-CH_3 \dots Cl^-$  is rapidly dissociated from  $FCH_3$  and  $Cl^-$  after the formation of complex II.

The dynamics calculations showed that the lifetime of complex I in the side-attack collision is significantly longer than in the collinear collision. Within its lifetime in the side-attack collision, the energy transfer from the excess energy of complex I to the internal modes of  $CH_3Cl$  has efficiently occurred. Therefore,

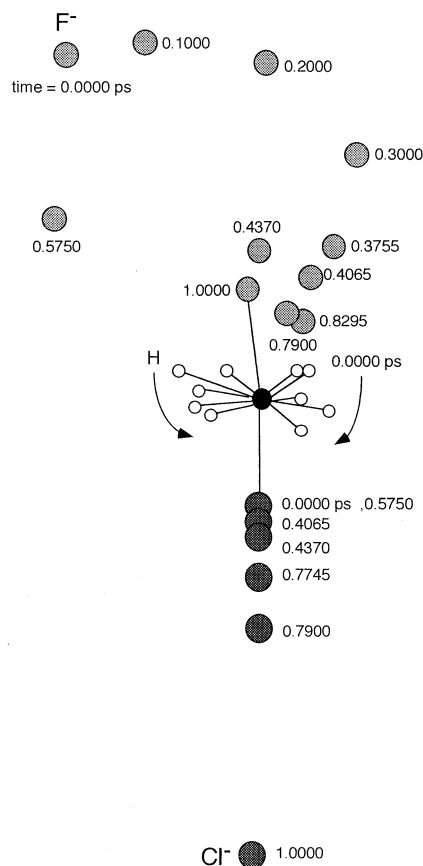


Fig. 4. Potential energy (A), interatomic distances (B), and angles vs. reaction time, calculated by the direct MO dynamics calculation (HF/3–21G+(*d*) level) for a side-attack collision of reaction (1).

the long lifetime of complex I causes the excitation of the C–F stretching mode and a lowering of the relative translational energy of products.

#### 4. Summary

In the present study we have examined several basis sets for the energetics, relative energies, and vibrational frequencies along the reaction coordinate of a  $S_N2$  reaction  $F^- + CH_3Cl \rightarrow CH_3F + Cl^-$  [reaction (1)]. From the ab initio MO calculations, it was shown that the HF/3–21+G(*d*) method gives a reasonable potential energy surface for reaction (1). CPU time for the dynamics calculation with this basis

set is significantly faster than the other basis sets such as 6–311++G(*d,p*). Therefore, the HF/3–21+G(*d*) level of theory is convenient for calculating the reaction dynamics.

The direct ab initio dynamics method at the HF/3–21+G(*d*) level was applied to reaction (1). Two collision angles (i.e. a near collinear collision and a side-attack collision) were examined in the calculations. In the collinear collision, the reaction proceeds by direct mechanism: the lifetimes of intermediate complexes are significantly short. The total available energy was mainly partitioned into a translational and the C–F stretching mode. The excitation of the C–F stretching mode would cause the excitation of the bending mode F–C–H by the internal energy redistribution. In the side-attack collision, it was found that the lifetime of complex I becomes longer, and the energy transfer to the internal mode of product occurred efficiently. More detailed calculations to elucidate the collision angle and collision energy dependence for reaction (1) are now in progress [25].

## Acknowledgements

The authors are indebted to the Computer Center at the Institute for Molecular Science (IMS) for the use of the computing facilities. We also acknowledge partial support from the Ministry of Education, Science, and Culture of Japan.

## References

- [1] See, for example, (a) M. Baer, in *The Theory of Chemical Reaction Dynamics*, M. Baer (Ed.) Chemical Rubber, Boca Raton, 1985, Vol. II, Chap. 4; (b) State-Selected and State-to-State Ion-Molecule Reaction Dynamics: Part I, Experiment, C.Y. Ng, M. Baer (Eds.) Vol. 82; *ibid.* Part II, Theory, M. Baer, C.Y. Ng (Eds.), in *Advances in Chemical Physics*, Wiley, New York, 1992.
- [2] (a) H. Tachikawa, *J. Chem. Phys.* 108 (1998) 3966; (b) H. Tachikawa, *J. Phys. Chem.* 100 (1996) 17090; (c) H. Tachikawa, *J. Phys. Chem.* 99 (1995) 255; (d) H. Tachikawa, T. Hamabayashi, H. Yoshida, *J. Phys. Chem.* 99 (1995) 16630; (e) H. Tachikawa, A. Murakami, *J. Phys. Chem.* 99 (1995) 11046; (f) H. Tachikawa, H. Takamura, H. Yoshida, *J. Phys. Chem.* 98 (1994) 5298.
- [3] (a) H. Tachikawa, *J. Phys. Chem. A* 102 (1998) 7065; (b) H. Tachikawa, *J. Phys. Chem. A* 101 (1997) 7475; (c) H. Tachikawa, *J. Phys. Chem.* 100 (1996) 17 090; (d) H. Tachikawa, K. Komaguchi, *Int. J. Mass Spectrom. Ion Processes* 164 (1997) 39; (e) H. Tachikawa, M. Igarashi, K. Komaguchi, *Int. J. Mass Spectrom. Ion Processes* 177 (1998) 17; (f) H. Tachikawa, M. Igarashi, *J. Chem. Phys.* 102 (1998) 8648; (g) Program code of the direct ab initio dynamics calculation was made by our group.
- [4] S.T. Graul, M.T. Bowers, *J. Am. Chem. Soc.* 113 (1991) 9696.
- [5] S.T. Graul, M.T. Bowers, *J. Am. Chem. Soc.* 116 (1994) 3875.
- [6] A.A. Viggiano, J.S. Paschkewitz, R.A. Morris, J.F. Paulson, A. Gonzalez-Lafont, D.G. Truhlar, *J. Am. Chem. Soc.* 113 (1991) 9404.
- [7] A.A. Viggiano, R.A. Morris, J.S. Paschkewitz, J.F. Paulson, *J. Am. Chem. Soc.* 114 (1992) 10 477.
- [8] M.V. Basilevsky, V.M. Ryaboy, *Chem. Phys. Lett.* 129 (1986) 71.
- [9] V.M. Ryaboy, *Chem. Phys. Lett.* 159 (1989) 371.
- [10] V.M. Ryaboy, in *Advances in Classical Trajectory Methods: Vol. 2, Dynamics of Ion-Molecule Complexes*, W.L. Hase (Ed.), JAI Press, Greenwich, CT, 1993, p. 115.
- [11] S.R. Vande Linde, W.L. Hase, *J. Am. Chem. Soc.* 111 (1989) 2349.
- [12] S.R. Vande Linde, W.L. Hase, *J. Phys. Chem.* 94 (1990) 2778.
- [13] S.R. Vande Linde, W.L. Hase, *J. Phys. Chem.* 94 (1990) 6148.
- [14] S.R. Vande Linde, W.L. Hase, *J. Chem. Phys.* 93 (1990) 7962.
- [15] Y.J. Cho, S.R. Vande Linde, L.H. Zhu, W.L. Hase, *J. Chem. Phys.* 96 (1992) 8275.
- [16] W.L. Hase, Y.J. Cho, *J. Chem. Phys.* 98 (1993) 8626.
- [17] W.L. Hase, *Science* 266 (1994) 998.
- [18] H. Wang, L. Zhu, W.L. Hase, *J. Phys. Chem.* 98 (1994) 1608.
- [16] H. Wang, G.H. Peslherbe, W.L. Hase, *J. Am. Chem. Soc.* 116 (1994) 9644.
- [19] G.H. Peslherbe, H. Wang, W.L. Hase, *J. Chem. Phys.* 102 (1995) 5626.
- [20] W.M. Olmstead, J.I. Brauman, *J. Am. Chem. Soc.* 99 (1977) 4219.
- [21] J.L. Duncan, A. Allan, D.C. McKean, *Mol. Phys.* 18 (1970) 289.
- [22] M.J. Frisch, G.W. Trucks, H.B. Schlegel, P.M.W. Gill, B.G. Johnson, M.A. Robb, J.R. Cheeseman, T. Keith, G.A. Petersson, J.A. Montgomery, K. Raghavachari, M.A. Al-Laham, V.G. Zakrzewski, J.V. Ortiz, J.B. Foresman, J. Cioslowski, B.B. Stefanov, A. Nanayakkara, M. Challacombe, C.Y. Peng, P.Y. Ayala, W. Chen, M.W. Wong, J.L. Andres, E.S. Replogle, R. Gomperts, R.L. Martin, D.J. Fox, J.S. Binkley, D.J. Defrees, J. Baker, J.P. Stewart, M. Head-Gordon, C. Gonzalez, J.A. Pople, Ab initio molecular orbital calculation program, GAUSSIAN 94, Revision D.3, Gaussian, Inc., Pittsburgh, PA, 1995.
- [23] J. Giguere, J. Overend, *Spectrochim. Acta A* 32 (1976) 241.
- [24] H. Wang, W.L. Hase, *J. Am. Chem. Soc.* 119 (1997) 3093.
- [25] M. Igarashi, H. Tachikawa, unpublished.